

Hydrothermal synthesis of rutile TiO₂ nanotubes film on Ti foil for photocatalytic degradation

Y. Sun^{a,b}, J. Qian^c, Q. R. Zhao^a, S. S. Yang^a, Y. Yang^a, Q. Zhao^{d,*}

^a*School of Mechanical Engineering, Chengdu University, Chengdu, 610106, China*

^b*Sichuan Province Engineering Research Center for Powder Metallurgy, Chengdu University, Chengdu, 610106, China*

^c*Institute of Optics and Electronics, Chinese Academy of Sciences, Chengdu, 610209, China*

^d*School of Chemical Engineering, Sichuan University, Chengdu, 610065, China*

One-dimensional TiO₂ nanotubes film was synthesized on the Ti foil oxidized at 800°C by hydrothermal method in a highly alkaline solution. The crystal structure, morphology and chemical state of the samples were characterized by X-ray diffraction, scanning electron microscope, transmission electron microscope and X-ray photoelectron spectroscopy. The result indicates that the TiO₂ nanotubes film still remains rutile phase structure after hydrothermal treatment. The growth mechanism of TiO₂ nanotubes is also discussed that includes dissolution, nucleation and growing process. The photocatalytic activity of TiO₂ film is remarkably improved after hydrothermal reaction. Due to the one-dimensional tubular structure, TiO₂ nanotubes film hydrothermally synthesized for 6 hours displays the highest photocatalytic degradation rate of methylene blue.

(Received January 7, 2021; Accepted May 1, 2021)

Keywords: Ti foil; TiO₂ nanotubes; Rutile; Hydrothermal; Photocatalytic degradation

1. Introduction

As a promising photocatalyst, TiO₂ has been widely applied in degradation of organic dyes [1-3]. Among many kinds of preparation methods, hydrothermal treatment can be regarded as a common and facile method to synthesize TiO₂ by using titanium alkoxides, TiO₂ powder, Ti powder and Ti foil as source materials [4-7]. In particular, various morphology structures of TiO₂, such as nanorods, nanosheets, nanowires, nanotubes and nanofibers [8-12], can be flexibly controlled via hydrothermal reaction parameters. Recently, TiO₂ nanotubes (TNTs) with large surface area have attracted many researchers' attention. However, the hydrothermal process is so complex and the growth mechanism of TiO₂ nanotubes is still ambiguous. Wu et al [13] and Chu et al [14] have reported the growth mechanism of TiO₂ nanotubes starting from anatase TiO₂ powder and Ti foil, respectively. To the best of our knowledge, there are few reports on the growth process of TiO₂ nanotubes prepared by hydrothermal method using rutile TiO₂ as starting material. In this

* Corresponding author: scuzq@scu.edu.cn

work, rutile phase TiO_2 was obtained by annealing Ti foil at 800 °C first and then the oxidized foil was hydrothermally treated with different times in NaOH solution to synthesize TiO_2 nanotubes. The formation of tubular structure from rutile phase TiO_2 was investigated through the morphology changes and the photocatalytic performance of TiO_2 nanotubes film was also discussed.

2. Experimental

Pure Ti foil (Alfa Aesar, 10 mm×60 mm×0.25 mm) was polished with a mixed solution of HNO_3 , HF and H_2O (volume ratio of 1:1:1), and then rinsed with deionized water. The dried Ti foil was oxidized in a muffle furnace at 800 °C for 4 h. Then the prepared sample was transferred into a 50 mL Teflon-lined stainless steel autoclave filled with 30 mL 10 M NaOH aqueous solution. The hydrothermal synthesis was carried out at 180 °C for different durations (1 h, 2 h, 4 h and 6 h). After cooling down to room temperature, the Ti substrate was immersed in 0.1 M HCl aqueous solution for 12 h and then washed with deionized water repeatedly. Finally, the samples were annealed in the muffle furnace at 450°C for 2 h, which were labeled as TNTs-1, TNTs-2, TNTs-4 and TNTs-6, respectively.

The crystal structure of product was tested by X-ray diffraction (DX 2700B, Dandong) using Cu Ka radiation. The morphology and microstructure of samples were observed by FESEM (Quanta 450, FEI) and transmission electron microscopy (JEM 2010 F, JEOL). The surface composition of the sample was examined by X ray photoelectron spectra (Escalab 250Xi, Thermo Scientific). Methylene blue (MB) was used as a pollutant to evaluate the photocatalytic activity of TiO_2 nanotube films under irradiation of a 350W Xenon lamp. Before irradiation, TiO_2 nanotube films (20 mm×10 mm) were immersed into 50 mL of MB aqueous solution (10 mg/L) under dark conditions for 30 min to reach adsorption/desorption equilibrium. The degradation rate of MB was measured by UV-Vis spectra recorded on UV-Vis spectrophotometer (UV-6100A, Shanghai Metash).

3. Results and discussion

Fig. 1 shows the XRD patterns of TiO_2 film calcined at 800°C, TiO_2 nanotubes film and Ti foil. It is clearly that the intensity of Ti peaks (JCPDS card No. 44-1294) is weakened dramatically and rutile (JCPDS card No. 65-0190) phase appears from the Ti substrate after calcining at 800°C for 4 h. The main peaks at $2\theta = 27.3^\circ, 35.9^\circ, 39.8^\circ, 41.1^\circ, 43.9^\circ, 54.2^\circ$ and 56.5° are indexed to (110), (101), (200), (111) (210), (211) and (220) planes.

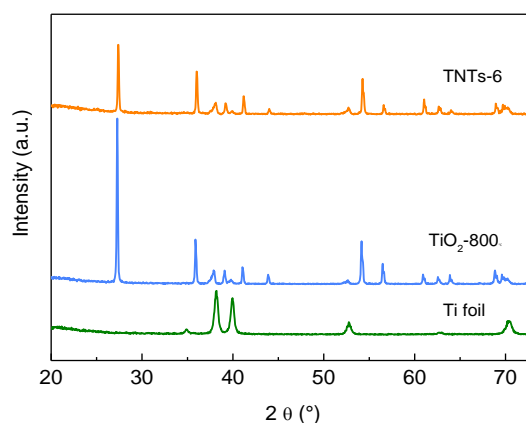


Fig. 1. XRD patterns of TiO_2 film calcined at 800°C and TiO_2 nanotubes film.

After the hydrothermal and calcination process, the XRD pattern of TiO_2 nanotube film is similar to that of the oxidized foil. According to Scherrer Formula [15], the average crystallite size of TiO_2 oxidized foil and TiO_2 nanotubes film is obtained, which is 53.9 nm and 49.0 nm, respectively. It is inferred that the rutile TiO_2 oxidized at 800°C can be regarded as a seed layer, subsequently nucleating and growing during the hydrothermal process. As the calcination temperature of TiO_2 nanotubes film is only 450°C so the average crystalline size is a little smaller.

Fig. 2 is the XPS spectra of TiO_2 nanotubes film to further investigate the elemental and chemical state of the sample. It can be seen in Fig. 2 (a) that the surface of the film is composed of Ti, O and a small amount of adventitious C elements.

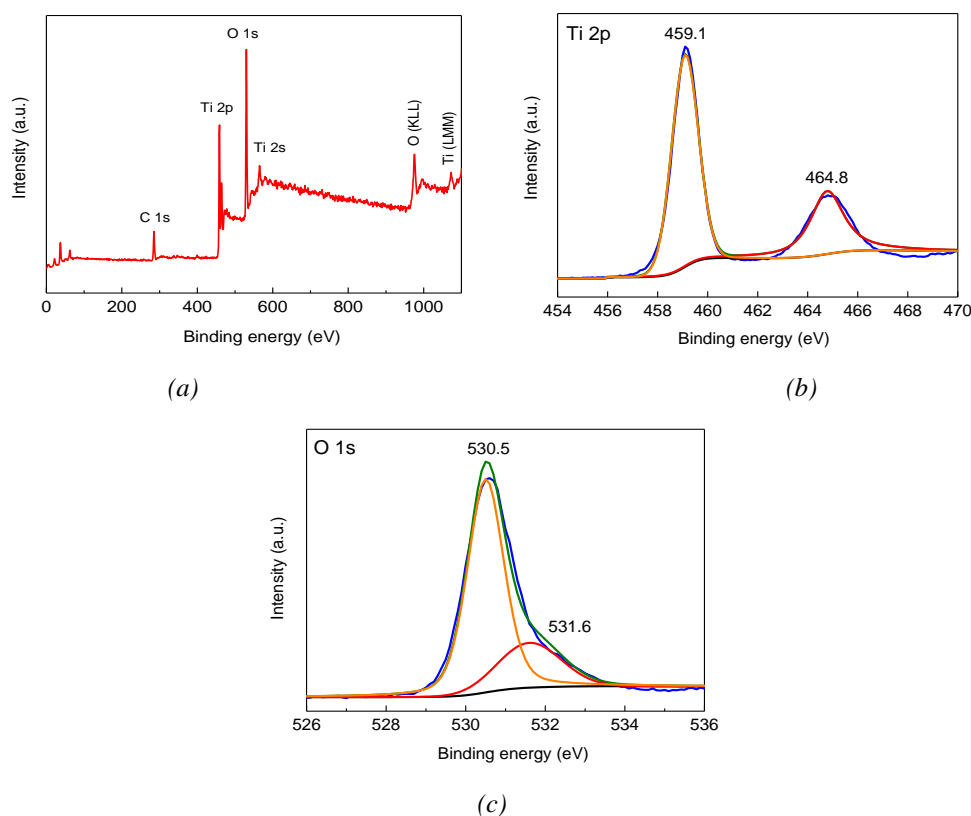


Fig. 2. XPS spectra of TiO_2 nanotubes film: (a) survey spectrum; (b) Ti 2p; (c) O 1s.

As shown in Fig. 2 (b), the two peaks at binding energies of 459.1 eV and 464.8 eV, corresponding to the Ti (2p 3/2) and Ti (2p 1/2) orbits, indicate the existence of Ti^{4+} state. Fig. 2 (c) displays the O 1s XPS spectrum. The two peaks at 530.5 eV and 531.6 eV are assigned to the lattice oxygen and surface adsorbed oxygen, respectively.

Fig. 3 demonstrates the growth of TiO_2 nanotubes film via SEM images of TiO_2 samples formed by different hydrothermal reaction times. Fig. 3 (a) shows the typical morphology of rutile TiO_2 . It is found that the oxidation film is uniform with TiO_2 particle size of nearly 200 nm after 800°C calcination. When the oxidized foil was hydrothermally treated for 1 h, the TiO_2 was dissolved to form a continuous ridge structure (Fig. 3 (b)).

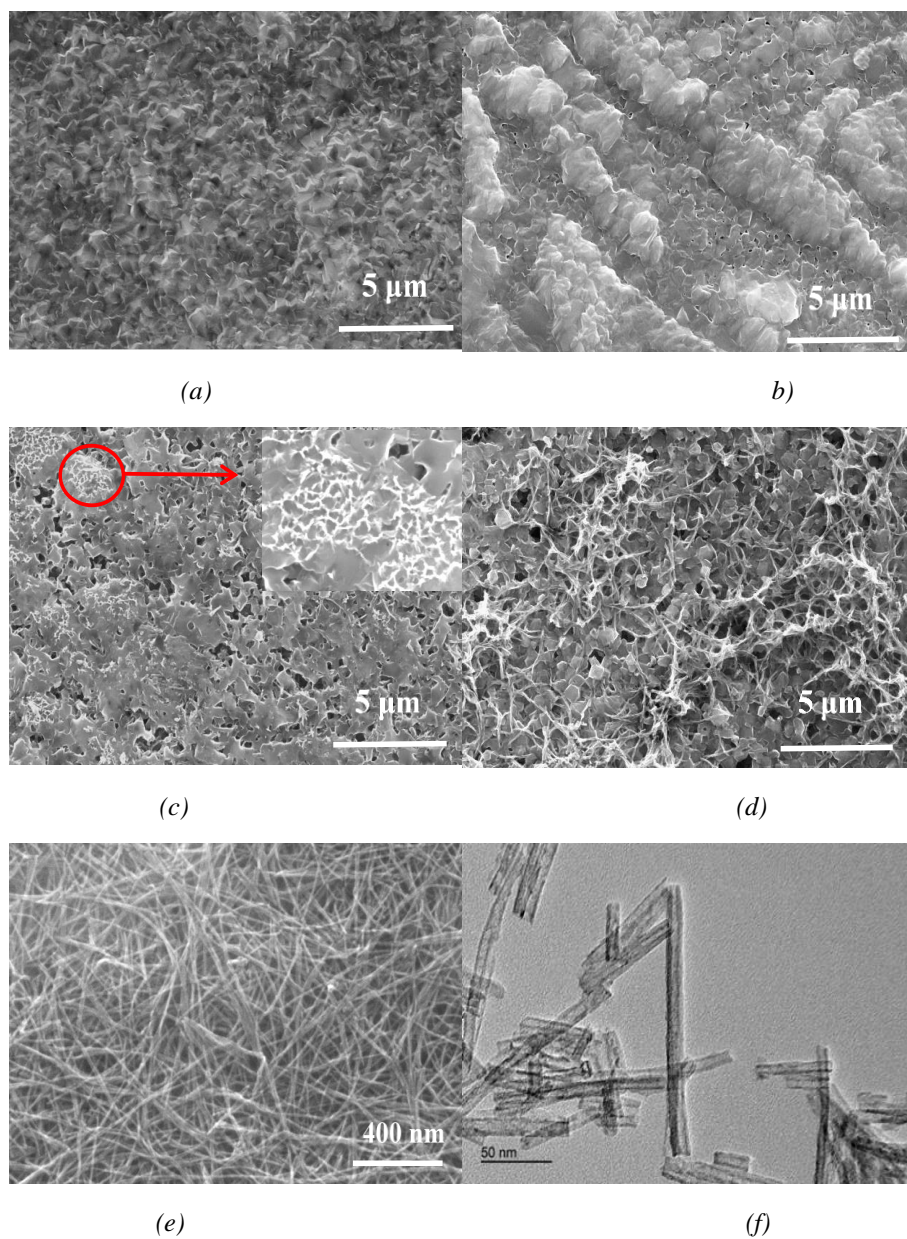


Fig. 3. SEM images of TiO_2 films: (a) calcined at 800 °C; (b) TNTs-1; (c) TNTs-2; (d) TNTs-4; (e) TNTs-6 and (f) TEM images of TNTs-6.

As the hydrothermal reaction time reaches 2 h (Fig. 3 (c)), the interlinked structure begins to appear on the TiO_2 surface. With increasing hydrothermal duration, the TiO_2 film is composed of nanosheets and more net structures (Fig. 3 (d)). As showed in Fig. 3 (e), the granulous surface of rutile TiO_2 has completely disappeared and the one-dimensional tubular structure with the length of several micrometers is observed when the oxidized foil was hydrothermally treated for 6 h. The diameter of the nanotubes can be measured by TEM images in Fig. 3 (f). It is clearly seen that the nanotubes film prepared in this work grew homogeneously with diameter of 10-15 nm.

The photocatalytic degradation rate of various TiO_2 film samples is compared in Fig. 4. For the TiO_2 film sample oxidized at 800°C , only 38.47% MB aqueous solution can be decomposed after 3 h of irradiation. After hydrothermal treatment from 1 h to 6 h, the photocatalytic degradation rate of MB over different photocatalysts is 40%, 45.79%, 53.39% and 66.59%, respectively. It is obvious that the photocatalytic activity of TiO_2 film can be improved via hydrothermal method. During the hydrothermal process, TiO_2 particles were dissolved in a highly alkaline environment and then formed nanotubes structure. TNTs-6 sample shows superior photocatalytic activity can be attributed to the one-dimensional tubular structure with large surface area and high charge transfer capability.

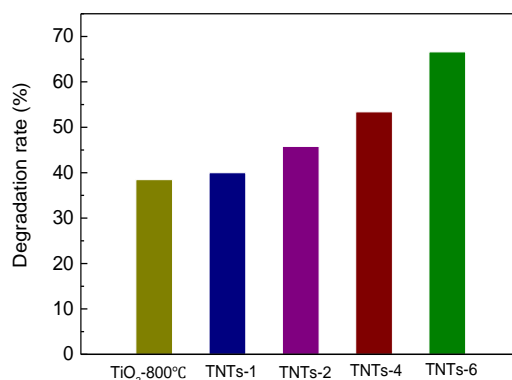


Fig. 4. Comparison of photocatalytic activity of various TiO_2 films.

4. Conclusion

Based on the Ti foil annealed at 800°C , one-dimensional TiO_2 nanotubes film was prepared via hydrothermal process. After hydrothermal treatment and calcination at 450°C , the TiO_2 nanotubes film remains rutile phase structure. The growth process of nanotubes structure from rutile TiO_2 on Ti foil is investigated by the morphology change of TiO_2 films prepared with different hydrothermal durations.

Comparing with TiO_2 film oxidized at 800°C , the photocatalytic activity of TiO_2 film evaluated by degradation of methylene blue under irradiation is significantly enhanced after hydrothermal process, which increases with the increasing hydrothermal reaction times. Due to the one-dimensional tubular structure, TiO_2 nanotubes film hydrothermally synthesized for 6 hours demonstrates higher photocatalytic activity than other samples.

Acknowledgments

This research is supported by the National Natural Science Foundation of China (No. 51702027) and Opening Foundation of Sichuan Province Engineering Research Center for Powder Metallurgy (SC-FMYJ2019-05).

References

- [1] R. Liu, Y. C. Bie, Y. J. Qiao, T. Liu, Y. J. Song, *Materials Letters* **251**, 126 (2019).
- [2] T. T. Yang, J. M. Peng, Y. Zheng, X. He, Y. D. Hou, L. Wu, X. Z. Fu, *Applied Catalysis B: Environmental* **221**, 223 (2018).
- [3] Y. Sun , Q. Liu , L. Zhu , Q. W. Tan , Y. X. Fan , B. S. Zhao, J. Guo, Q. Q. Kong, *Digest Journal of Nanomaterials and Biostructures* **14**, 139 (2019).
- [4] G. C. Park, T. Y. Seo, C. H. Park, J. H. Lim, J. Joo, *Industrial & engineering chemistry Research* **56**(29), 8235 (2017).
- [5] S. H. Cho, G. Gyawali, R. Adhikari, T. H. Kim, S. W. Lee, *Materials Chemistry and Physics* **145**(3), 297 (2014).
- [6] F. Zuo, K. Bozhilov, R. J. Dillon, L. Wang, P. Smith, X. Zhao, C. Bardeen, P. Y. Feng, *Angewandte Chemie* **51**(25), 6223 (2012).
- [7] H. C. Lin, X. Li, X.Y. He, J. B. Zhao, *Electrochimica Acta* **173**, 242 (2015).
- [8] D. J. Yan, J. K. Liu, Z. C. Shang, H. A. Luo, *Dalton Transactions* **46**, 10558 (2017).
- [9] J. G. Yu, J. X. Low, W. Xiao, P. Zhou, M. Jaroniec, *Journal of the American Chemical Society* **136**(25), 8839 (2014).
- [10] Y. P. Tang, L. Hong, Q. L. Wu, J. Q. Li, G.Y. Hou, H. Z. Cao, L. K. Wu, G. Q. Zheng, *Electrochim Acta* **195**, 27 (2016).
- [11] Q. Luo, Q. Z. Cai, X. W. Li, X. D. Chen, *Journal of Alloys and Compounds* **597**, 101 (2014).
- [12] M. C. Wu, P. Y. Wu, T. H. Lin, T. F. Lin, *Applied Surface Science* **430**, 390 (2018).
- [13] D. Wu, J. Liu, X. N. Zhao, A. D. Li, Y. F. Chen, N. B. Ming, *Chemistry of materials* **18**(2), 547 (2006).
- [14] M. S. Chu, Y. L. Tang, N. N. Rong, X. Cui, F. L. Liu, Y. H. Li, C. Zhang, P. Xiao, Y. H. Zhang, *Materials & Design* **97**, 257 (2016).
- [15] V. Uvarov, I. Popov, *Materials Characterization* **58**(10), 883 (2007).